Radiol Oncol 1996; 30: 291-97.

Monte Carlo Simulations of a metal/a-Se Portal Detector

Hui Wang, B. Gino Fallone, Tony Falco

Medical Physics Unit and Department of Physics, McGill University and Montreal General Hospital, Montreal, Quebec, Canada

The detector response, modulation transfer function (MTF) and quantum detective efficiency (DQE) of four amorphous selenium (a-Se) based image receptors have been calculated through Monte Carlo simulations of x-ray absorption. As part of a preliminary study on electrostatic portal imaging, the effects of receptor geometry and composition on the imaging characteristics of a-Se in the megavoltage range have been investigated. Our results indicate that the DQE increases as the a-Se thickness while the MTF decreases slightly, and a front metal plate can enhance detector response, DQE and MTF of a-Se receptors at the detail level relevant to portal imaging.

Key words: Monte Carlo method, portal detector; selenium; radiography-methods, metal/a-Se detector

Introduction

Electrostatic (xeroradiographic) imaging is a process in which the intensity pattern of a photon beam is transformed to a charge distribution on the surface of a photoconductor.[1-2] With the development of novel methods for extracting the latent image, such as photoinduced discharge with laser[3-5] and electrostatic coupling, xeroradiography is regaining its vitality. Recent studies have shown that by using amorphous Selenium (a-Se) and digital readout has various advantages: higher contrast, wider dynamic range and improved quantum detective efficiency.[6,7] A latent image on the a-Se surface is formed via local neutralization of the uniform charge distribution achieved through some charging procedure before irradiation. In diagnostic radiology, the selenium is directly exposed to x-rays transmitted through a patient. One would naturally ask if a-Se can be introduced into portal imaging where beam energy is much higher.

Correspondence to: Prof. Gino Fallone, Ph.D., FCPM, ABMP, Medical Physics Unit and Department of Physics, Mc Gill University and Montreal General Hospital, 1650 Cedar Avenue, Montreal, Quebec H3G 1A4, Canada.

UDC: 616-073.75:530.145:591.283

In portal imaging, an image is acquired with a therapy beam with high penetrating ability which reduces detection efficiency. A metal plate is usually combined with a portal image receptor. For example, a portal film is placed in a cassette with a copper plate on the beam entrance side. Because of the high attenuation coefficient of the metal, a significant portion of the incident photon beam is converted to secondary electrons. It is the interaction of the electrons with the receptor that is responsible for image formation. Metal plates are also employed in fluoroscopic EPIDs and matrix ion chamber EPIDs to enhance detector response.

Droege and Bjarngard reported that a metal plate can significantly reduce scatter to primary ratio when used with portal films.[8] Jaffray et al reported that a copper plate can reduce quantum noise associated with x-ray absorption in phosphor screens thus improve the detective quantum efficiency.[9]

The objective of this study is to measure the radiation discharging curve of metal/a-Se receptors, and to calculate their detector response, modulation transfer function and the detective quantum efficiency in the megavoltage range with the Monte Carlo technique.

Mathematical simulations

Theory

The measurement of the line spread function $l(x)$ can be modelled as a smoothing process followed by sampling process. Mathematically, the measured line spread function $l_m(x)$ can be expressed as

$$l_m(x) = \left[l(x) \otimes rect\left(\frac{x}{a}\right)\right] \cdot comb\left(\frac{x}{b}\right)$$

where the convolution with

$$rect\left(\frac{x}{a}\right) = \begin{cases} 1, & |x \le \frac{a}{2}| \\ 0, & |x > \frac{a}{2}| \end{cases}$$

represents the averaging effect of the aperture size a, and the multiplication with

$$comb\left(\frac{x}{b}\right) = \sum_{n=-\infty}^{n=+\infty} \delta(x - nb)$$

represents the sampling with a spacing of b. The measured modulation transfer function is then given by the modulus of the Fourier transform of $lm(x)$:

$$MTF_m(u) = |\mathcal{F}\{l_m(x)\}|$$
$$= |[MTF(u) \cdot sinc(au)] \otimes comb(bu)|$$

which contains truncation error introduced by the multiplication with $sinc(au)$ and aliasing artifact introduced by the convolution with $(comb(bu))$. Precautions have to be taken in the selection of aperture size and sampling rate in order to keep systematic errors under an acceptable limit. The upper limit of spatial frequency at which the modulation transfer function can be measured is determined by the Nyquist criterion:

$$u_{max} = \frac{1}{2b}.$$

The convolution in Eq. (4) causes overlapping of adjacent cycles. This overlap can be reduced by increasing the aperture size. A larger aperture reduces the amplitudes of the sidelobes of $sinc(au)$ but at the same time increases truncation error. As a trade-off of aliasing reduction, the measured modulation transfer function will deviate more from the true value. The current convention used in modulation transfer function measurements is $a = 2b$, i.e., the aperture should be at least twice the size of the sampling interval. This convention ensures a less than 2 % systematic error in the sampled data.[10]

Quantum noise in x-ray imaging originates from the fluctuation of the incident photon flux characterized by Poisson statistics and the randomness of the amount of energy deposited by each x-ray photon in the receptor. While the former determines the noise level of the input, the latter is the reason for the degradation of the signal to noise level introduced by the receptor. This degradation is usually characterized by the detective quantum efficiency defined as

$$DQE = \left(\frac{SNR_{out}}{SNR_{in}}\right)^2.$$

For an amorphous selenium receptor, the energy deposited by an incident photon is used to create electron-hole pairs which are responsible for the formation of the electrostatic image. The number of these charge carriers resulted from E incident photons of energy is given by

$$\frac{\int_0^{E_{in}} n(E, E_{in}) E dE}{W}$$

where $n(E, E_{in})$ is the average number of photons that deposited the amount of energy E and W is the average energy required to generate one electron-hole pair. The fluctuation of $n(E, E_{in})$ is $\sqrt{n(E, E_{in})}$. Considering the absorbed energy distribution, the total uncertainty is

$$\frac{\sqrt{\int_0^{E_{in}} \left(\sqrt{n(E, E_{in})}E\right)^2 dE}}{W}.$$

Therefore,

$$SNR_{out} = \frac{\int_0^{E_{in}} n(E) E dE}{\sqrt{\int_0^{E_{in}} n(E) E^2 dE}}$$

$$SNR_{in} = \frac{N}{\sqrt{N}}$$

$$DQE = \left(\frac{\int_0^{E_{in}} \frac{n(E, E_{in})}{N} E dE}{\sqrt{\int_0^{E_{in}} \frac{n(E, E_{in})}{N} E^2 dE}}\right)^2$$
$$= \frac{M_1^2(E_{in})}{M_2(E_{in})}$$

where

$$M_i(E_{in}) = \int_0^{E_{in}} \frac{n(E, E_{in})}{N} E^i dE$$

is the ith moment of the normalized pulse height spectrum $\frac{n(E,E_{in})}{N}$ from incident photons of energy E_{in}. Eq(11) is the DQE at zero spatial frequency because spatial information transfer is not considered. DQE at a non zero spatial frequency is lower as the receptor can not fully transfer the information at that detail level. DQE as a function of spatial frequency can be expressed as

$$DQE(f) = DQE(0) \cdot MTF^2(f)$$

provided that quantum noise is white noise. This is justifiable since the input noise is determined by the Poisson statistics and the output noise is determined by the fluctuation in the energy deposited by a photon. Neither of them depends on the spatial frequency of the input under the assumption that x-rays are photons and the detector is a large continuum.

Monte Carlo Simulations

Image acquisition in transmission radiology starts with the detection of x-rays transmitted through a patient. The change of some physical observable caused by the interaction between the x-rays and the detector is then extracted as the output signal by a certain means. The incident photon generates a photon-electron "shower" in the detector introducing an uncertainty in the spatial location of the incident point resulting in receptor blur. Due to the stochastic nature of the coupled photon-electron transport, energy deposition introduces fluctuation in the output signal or quantum noise.[11-13] The magnitude of receptor blur and quantum noise depend on the energy of the x-rays and the composition and geometry of the receptor.

The coupled photon-electron transport within the detector was simulated with the Electron Gamma Shower (EGS4) code[14] which has been extensively used for radiation dose calculation in the energy range of 1~10 MeV and has been proven to produce reliable results. As a general purpose software package, EGS4 (National Research Council, Canada) consists of two major parts: the system code that handles the physics of coupled photon-electron transport and the user code that defines the geometry and type of the medium/media. The user code also specifies which physical observable(s) will be scored. This package also provides two general purpose programs, XYZDOS and DOSRZ, to define simulation geometry in Cartesian and polar coordinate systems which include the Parameter Reduced Electron Step Transport Algorithm (PRESTA) that reduces the dependence of charged particle transport on user-selected parameters.[15] Density effect corrections were also included in the collisional stopping powers. The K fluorescence production was not considered since it is not significant in the megavoltage energy range.[9] The parameters controlling the transport were set as the following: ECUT=AE=0.521 MeV, PCUT=AP=0.01 MeV, where ECUT is the minimum total energy of electrons that are transported, PCUT is the minimum total energy of photons that are transported, AE and AP are the energy thresholds for creation of secondary electrons and photons, respectively. Monoenergetic photons (0.1~6 MeV) were used in all simulations. The results of simulation runs are consistently well within 1 % of each other.

A layer of amorphous selenium is coated on an 8 x 8 in^2 metal plate: the metal-plate is in the beam-entrance side of the detector. As a build up material, the metal plate converts the incident photons into electrons. Intuitively, the optimal thickness of the metal plate should be the depth d_{max} where electron equilibrium is reached. Beyond this depth, energy absorption decreases because the primary photon beam is attenuated and electrons do not travel over a certain range. Three of the four receptors (Noranda Advanced Materials Inc., Pointe Claire, QC) have a 2 mm thick aluminum plate with different thickness of a-Se: 150 μm, 300 μm and 500 μm. The other receptor consists of 1 mm copper and 300 μm a-Se.

The simulation of the line spread function was run with the user code XYZDOS. A 2 μm x 20 cm^2 parallel beam of monoenergetic photons is incident at the center of a 20 x 20 cm^2 receptor. The a-Se layer of the receptor is divided into a series of 5 μm wide strips inside which the deposited energies are scored. Every two adjacent points are then averaged:

$$l_m(x_i) = \frac{1}{2}[E(x_i) + E(x_{i+1})]$$
$$x_i = (i-1)h, \quad i = 1, 2, 3, \cdots, N.$$

to satisfy the requirement of the adequate aperture size. According to the Nyquist criterion, the sampling rate gives a cutoff frequency of 100 mm^{-1}. The selection of the bin width must also ensure that multiple scattering can be modelled accurately by the EGS4 Monte Carlo code. The rule of thumb to estimate the number of multiple scattering events is

$$N_{ms} = density(g/cm^3) \cdot (Z/8)^{\frac{1}{3}} \cdot stepsize(\mu m).$$

where N_{ms} is the number of multiple scattering events, Z is the atomic number of the material considered. For a 5 μm step size in amorphous selenium, N_{ms} is approximately 35 which is sufficient. The MTF is obtained by applying the Fast Fourier Transform (FFT) to the discrete LSF. To ensure the accuracy of the results, 30 millions of photons were used in each simulation resulting in a statistical uncertainty less than 5 % in each strip. This requires calculation times ranging from 7 to 24 hours on an SGI workstation (IRIS INDIGO, Silicon Graphics, Mountainview, CA).

In order to calculate the absorption efficiency and the detective quantum efficiency, the energy absorbed in the entire sensitive volume and its pulse height spectrum need to be scored. Unfortunately, XYZDOS does not include the option of pulse height spectrum. The simulations had to be run with the more versatile and more user friendly DOSRZ. A pencil beam of monoenergetic photons is incident at the center of the circular detector with a radius of 10 cm. The effect of the detector shape is negligible since the radius is sufficiently large for a pencil beam. Equal energy bin width was used in the pulse height spectrum: 0.01 MeV for incident photons of energy less than 3 MeV and 0.03 MeV for 3 MeV and above. Simulation were terminated only when the uncertainty in the pulse height spectrum became less than 10 % in each bin. Approximately 72 hours were required for each run.

Results

Three of the four receptors have a common front metal plate (2 mm Al) but different a-Se layer (150 μm, 300 μm and 500 μm thick) while the other has a 1 mm thick Cu front plate and 300 μm thick a-Se. The calculated MTFs are shown in Figure 1. Error bars are not plotted because they are smaller than the symbols.

For each plate, the MTF degrades as energy increases and becomes relatively constant from 2 MeV up to 6 MeV. This indicates that there is a transition of the dominant interaction from one type to another between 1 and 2 MeV. The MTFs were also calculated for the a-Se/Cu receptor when the Cu plate was used as back plate. Degradation was also observed as the photon energy was increased.

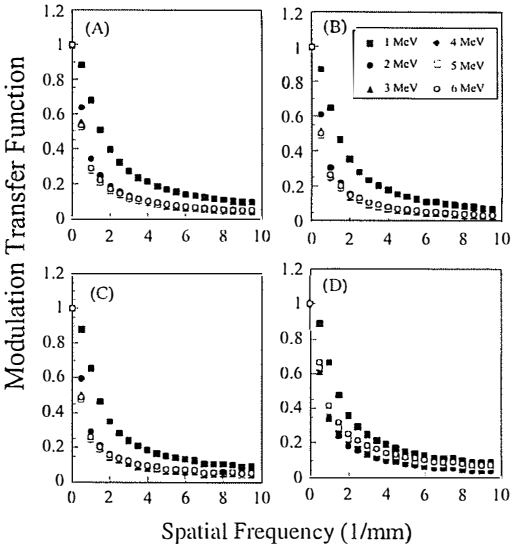

Figure 1. The modulation transfer functions for different energies for various receptors (A) 2 mm Al/0.15 mm a-Se, (B) 2 mm Al/0.30 mm a-Se, (C) 2 mm Al/0.50 mm a-Se, (D) 1 mm Cu/0.3 mm

The data of all receptors at each individual energy were plotted in Figure 2. It can be seen that for the Al plate receptors, the MTF decreases as the thickness of the a-Se increases at all energies (1~6 MeV). For 300 μm thick a-Se layer, a 2 mm Al plate and a 1 mm Cu plate lead to the same modulation transfer function at 1 MeV. As the photon energies increases, the Cu plate improves the MTF considerably. When a back Cu plate is used, the MTF is the lowest at 1 MeV but highest for 2 MeV and above.

The quantum absorption efficiency is defined as the ratio of the photons that have deposited energy in the sensitive volume of the detector to all the incident photons. Figure 3 (A) shows the calculated quantum absorption efficiencies of four receptors. The error bars are too small to be shown in the plots. The quantum absorption efficiency increases as the a-Se layer becomes thicker when the same front plate is used. At 1 MeV, a front metal plate reduces the probability of absorption due to the attenuation of the primary beam. For energies ≥ 2 MeV, the 1 mm Cu front plate increases the absorption more than the 1 mm Cu back plate. A 1 mm Cu back plate is more effective in absorption than a 2 mm Al front plate.

The output signal of a receptor is determined by the average energy deposited by an incident photon. Figure 3 (B) shows the responses of four receptors to

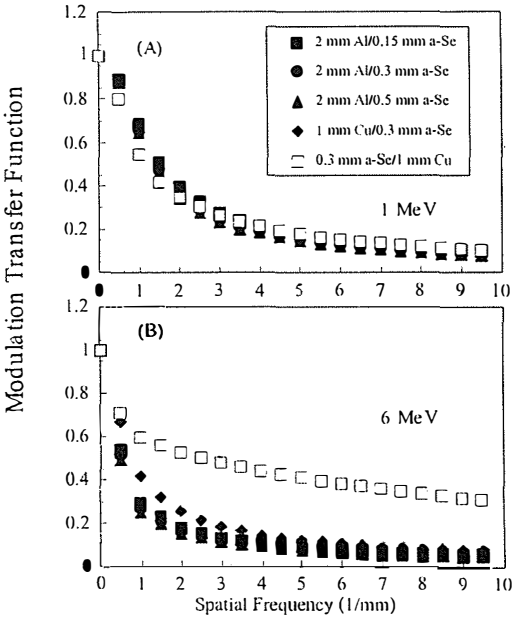

Figure 2. The modulation transfer functions of four receptor at incident photon energy of (A) 1 MeV and of (B) 6 MeV.

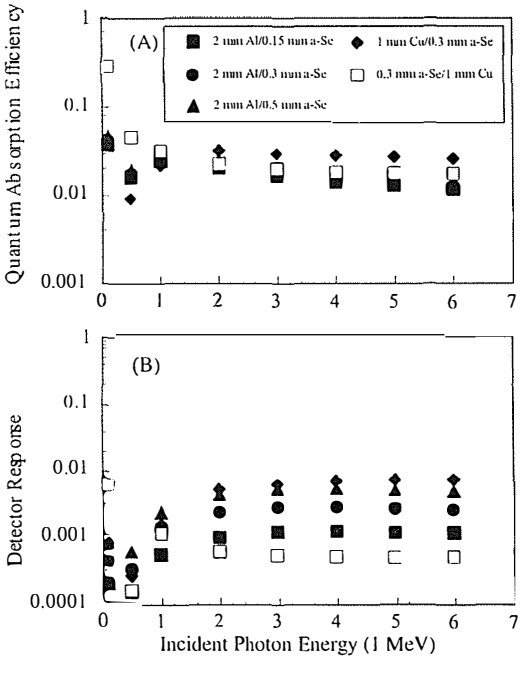

Figure 3. (A) Quantum absorption efficiencies and (B) Detector response of four receptors at different incident photon energies.

monoenergetic photons at different energies. For the three Al plates, detector response increases with the thickness of a-Se. For the same thickness of the a-Se layer (300 μm), a 1 mm Cu front plate results in a much greater detector response than a 2 mm Al front plate. The comparative detector response of the Cu with respect to Al increases at higher energies. For 2 MeV and above, it becomes even greater than that of the Al receptor with a thicker a-Se layer (500 μm). Among all the receptors, the one with a 1 mm Cu back plate has the lowest detector response.

The statistical factor describes the loss in DQE due to the incomplete absorption of an interacting photon. As shown in Figure 4 (A), the statistical factor of a front metal plate receptor decreases as the x-ray energy increases. With the front metal plate as an electron convertor, the pulse height spectra of energy deposition in the a-Se layer have similar shapes at different energies. But the width increases with energy. The drop of the statistical factor is due to this widening. For a back metal-plate receptor, however, the pulse height spectrum becomes narrower when x-ray energy increases. The smaller variation in the amount of the energy deposited per interaction photon is responsible for the slight increase of the statistical factor of the 1 mm Cu back plate receptor.

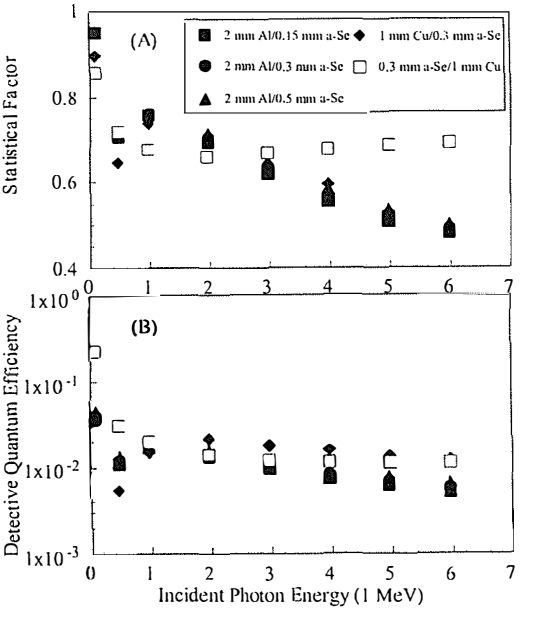

Figure 4. (A) Statistical factors, and (B) Zero spatial frequency detective quantum efficiencies of four receptors at different incident photon energies.

The zero spatial frequency DQE of the four receptors are shown in Figure 4 (B). Except for the 1 mm Cu receptor at 1 MeV, the DQEs of all four receptors decrease as incident photon energy increases. For the same front metal plate, a larger sensitive volume results in a higher DQE due a more complete absorption of the incident photon. For the same a-Se layer, a front metal plate decreases the DQE at 1 MeV due to the attenuation of the primary photons (Figure 3 (A)). But for 2 MeV and above, the 1 mm Cu front plate, increases the DQE more than the 2 mm Al front plate. Figures 3, 4 (A) and (B) indicate that DQE is dominated by quantum absorption efficiency. The DQE as a function of spatial frequency can be calculated from Eq(13). For 2 MeV and above, both the zero frequency DQE and the MTF of the Cu receptor are greater than those of the Al receptor. The Cu front plate, therefore, will lead to higher DQE at any detail level. At 1 MeV, the DQE of the Cu receptor at higher spatial frequencies will be compensated by its higher MTF.

Discussion

Image formation in a xeroradiograhic system has three stages: x-ray absorption, electron-hole pair production and charge collection. In our simulations, only the first is modeled. Another simplification is that only monoenergetic x-ray beams were considered.

Our calculations of zero frequency DQEs have followed the approach taken by Jaffray *et al*[9] to calculate zero frequency DQEs of metal plate/phosphor screen combinations. Since the physical process modeled by the simulations is the same: energy absorption, the results could be compared. In fact, similar trends are observed in the way zero frequency DQE changes with respect to incident photon energy although the behavior of the DQE(●) of the metal plate/a-Se detector is not as simple. Since the Monte Carlo results are the higher limit, comparison of the overall performance of the two type of detection systems (metal/a-Se versus metal/phosphor) must include the later stages in the imaging chain. The metal/phosphor system requires an additional component that converts light into an electronic signal which may seriously affect the resultant DQE. This critical component is theoretically not required for metal/a-Se system, where the information is already stored in charge form. Intuitively, it should be simpler to read charge information directly in the metal/a-Se system than it would be with a metal/phosphor system. However, the optimum technique for reading a metal/a-Se has not been found yet.

References

1. Boag JW. Xeroradiography. *Physics in Medicine and Biology* 1973; **18:** 3-37.
2. Brodie I and Gutcheck RA. Minimum esposure estimates for information recording in diagnostic radiology. *Medical Physics* 1985; **12:** 362-7.
3. Zermeno A, Kirby T, Cowart R, Marsh L and P. Ong. Laser readout of electrostatic images. *Application of Optical Instrumentation to Medicine VII, Proceedings of SPIE* 1979; **173:** 81-7.
4. Cook EL, Edwards JD, Nelson OL and Potts JE. *Performance of a high resolution radiographic detector.* The society of Imaging Science and Technology 47th Annual Conference ICPS 1994; 699 .
5. Rowlands JA and Hunter DM. X-ray imaging using amorphous selenium: Photoindeced discharge (PID) readout for digital general radiography. *Medical Physics* 1995; **22:** 1983-2005.
6. Brodie I and Gutcheck RA. Radiographic information theory and application to mammography. *Medical Physics* 1982; **9:** 79-94.
7. Neitzel U, Maack I and Gunther-Kohfahl S. Image quality of a digital chest radiography system based on a selenium detector. *Medical Physics* 1994; **21:** 509-16.
8. Swank R. Absorption and noise in x-ray phosphors. *Journal of Applied Physics* 1873; **44:** 4199-203.
9. Swank R. Measurement of absorption and noise in an x-ray image intensifier. *Journal of Applied Physics* 1974; **45:** 3673-8.
10. Dick CE and Motz JW. Image information transfer properties of x-ray image intensifiers. *Medical Physics* 1981; **10:** 337-46.
11. Droege RT and Bjarngard B. Influence of metal screens on contrast in megavoltage x-ray imaging. *Medical Physics* 1979; **6:** 515-8.
12. Jaffray DA, Battista JJ, Fenster A and Munro P. Monte Carlo studies of x-ray energy absorption and quantum noise in megavoltage transmission radiography. *Medical Physics* 1995; **22:** 1077-88.
13. Villafana T. Modulation transfer function of a finite scanning microdensitometer slit. *Medical Physics* 1975; **2:** 251-4.
14. Rogers DWO and Bielajew AF. Monte Carlo techniques of electron and photon transport for radiation dosimetry. *The Dosimetry of Ionizing Radiation* III Academic Press, 1990.
15. Bielajew AF and Rogers DWO. PRESTA – The Parameter Reduced Electron-Step Transport Algorithm for Electron Monte Carlo Transport. *Nuclear Instruments and Method B* 1984; **18:** 535-48.